Finite Elements in Analysis and Design 7 (1991) 317–324
Elsevier

Structural optimization including centrifugal effects

Howard D. Gans

Department of Aeronautics and Astronautics, Air Force Institute of Technology, Wright-Patterson Air Force Base, OH 45433, USA

William J. Anderson

Department of Aerospace Engineering, University of Michigan, Ann Arbor, MI 48109, USA

Revised July 1990

Abstract. This paper investigates the effects of centrifugal forces on the frequencies of a rotating system and then provides an optimal redesign process. The rotational effects have a profound influence on the eigenfrequencies and are important in optimal structural redesign where the frequencies must be adjusted. The optimal redesign is done by deriving nonlinear inverse perturbation equations for the problem. Structural changes typically meet the frequency goals to within three percent.

Introduction

The desire to minimize weight while meeting design requirements is a key concept in optimal structural design. In any structural redesign problem, there are several possible candidate designs that would meet the new criteria. The objective function for redesign may be quite different from the objective function in the original design of a part. It may be necessary to obtain the optimal design that requires the least possible change from the original design in terms of some dimension, such as thickness. This is a "minimum change" criterion for optimization.

Some structures are subject to body forces in addition to loadings caused by boundary forces. Rotating bodies experience centrifugal effects. In a rotating frame, the centrifugal effects may be viewed as a reverse-effective pseudo-force. If the rotational speed is small enough, these forces can be neglected. In high speed applications, however, centrifugal forces can result in stiffening. This introduces a nonlinearity in a classical analysis sense.

The objective of this study is to first solve for the stiffening effect of the centrifugal force and to calculate the mode shapes and frequencies of a structure composed of several types of elements. Then, nonlinear inverse perturbation will be used to account for the stiffening effect as the redesign progresses. This scheme measures design changes as perturbations of the original structure. The method will be applied to a problem involving a typical curved compressor blade. Coriolis effects are not included in this paper but have been considered separately.

Theoretical overview and solution procedure

Motion of rotating system

For the free vibration problem involving no damping or gyroscopic effects, the equation of motion of the discretized system may be expressed by:

$$[M]\{\ddot{u}\} + [K]\{u\} = \{0\}. \tag{1}$$

Elsevier Science Publishers B.V.

Solutions admit n eigenvalues ω_i and n associated eigenvectors $\{\phi\}_i$ where n represents the number of degrees of freedom. The lowest eigenvalue, ω_1, is the fundamental frequency which typically is a bending mode. The corresponding mode shape is $\{\phi\}_1$.

In the total optimization approach, the forward problem encompasses the modal analysis of the rotating structure. This can be thought of as a free vibration problem, with a centrifugal force acting as a stiffening effect. This can be quantified by examining the nonlinear components of the structural stiffness matrix.

In nonlinear analysis, the stiffness matrix is represented by $[K_T]$ which is a tangent matrix such that:

$$[K_T] = [K_0] + [K_D] + [K_L], \tag{2}$$

where $[K_T]$ is the tangent stiffness matrix, $[K_0]$ is the small-displacement stiffness matrix, $[K_D]$ is the differential stiffness matrix (often called geometric stiffness or initial stress matrix), and $[K_L]$ is the large-displacement matrix.

In solving the rotating problem, it is assumed that displacements are small; therefore, $[K_L]$ is neglected in eqn. (2). The differential stiffness matrix, which is retained, does not explicitly contain displacements, but is dependent on the stress level. The matrix $[K_0]$ is given by Zienkiewicz [1] and others. Furthermore, it can be shown [2] that for a beam:

$$[k_D^e] = \int_V [N']^T \begin{bmatrix} [s] & [0] & [0] \\ [0] & [s] & [0] \\ [0] & [0] & [s] \end{bmatrix} [N'] \, dV \tag{3}$$

where $[k_D^e]$ is the element differential stiffness matrix, $[N']$ is the spatial derivative of the shape function matrix, and $[s]$ is the matrix of applied stresses such that:

$$[s] = \begin{bmatrix} \sigma_{x0} & \tau_{xy0} & \tau_{xz0} \\ \tau_{xy0} & \sigma_{y0} & \tau_{yz0} \\ \tau_{xz0} & \tau_{yz0} & \sigma_{z0} \end{bmatrix}. \tag{4}$$

Nonlinear inverse perturbation method

The predictor–corrector method for structural optimization employing nonlinear inverse perturbation was developed by Hoff et al. [3], based on the work by Stetson [4], Stetson and Palma [5], and Sandström and Anderson [6]. This method was expanded to rotating structures by Gans [7].

The predictor–corrector method will be developed by the use of a simple rotating cantilevered beam as shown in Fig. 1. The first design change seeks a 10% increase in the fundamental flexural model frequency. In the predictor step, we will assume that the element change α_e is small; therefore, the quantity $(1 + \alpha_e)^3 - 1$ may be approximated by $3\alpha_e$. This results in a 3.11% error, but is done so as to facilitate solving for α_e, which we shall see is the unknown in the inverse perturbation scheme.

The element change property α_e is given by:

$$\alpha_e = \Delta t_e / t_e, \tag{4}$$

where t_e is the element thickness and Δt_e is the change in element thickness. Thickness for the beam in Fig. 1 is in the z-direction in the cross section. Let M_i be the generalized mass for the ith mode, ω_i be the eigenfrequency and $[k_{e_{\text{memb}}}]$, $[k_{e_{\text{diff}}}]$, $[k_{e_{\text{bend}}}]$ and $[m_e]$ be the element membrane stiffness, differential stiffness, and bending stiffness and mass matrices, respectively.

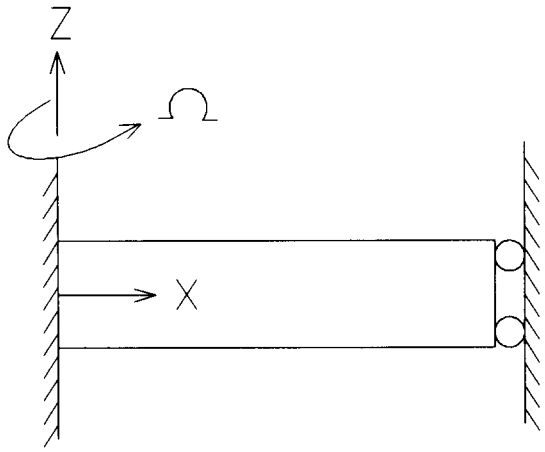

Fig. 1. Rotating beam.

Therefore, the scalar equation that gives the relationship between α_e and the desired change in natural frequency $\Delta\omega_i$ including centrifugal effects is given by:

$$\Delta(\omega_i^2) = M_i^{-1} \sum_{e=1}^{p} \left[\{\psi\}_i^{\mathrm{T}} \left(\left[k_{e_{\mathrm{memb}}}\right] + \left[k_{e_{\mathrm{diff}}}\right] + 3\left[k_{e_{\mathrm{bend}}}\right] \right) \{\psi\}_i \alpha_e - \omega_i^2 \{\psi\}_i^{\mathrm{T}} [m_e] \{\psi\}_i \alpha_e \right], \tag{5}$$

where the approximation of the expansion of $(1 + \alpha_e)^3$ as $3\alpha_e$ is applied.

The above equation is called the *predictor*. It relates the element changes to a prescribed change in the desired eigenfrequency. In this way, the equation predicts what the system configuration should be for a given amount of frequency change.

Using the results from the static analysis, one finds the eigenvalues and eigenvectors for the rotating system by finite element modal analysis using MSC/NASTRAN as modified with Direct Matrix Abstraction Programming (DMAP). Then, eqn. (5) is used as an equality constraint in the Augmented Lagrange Multiplier (ALM) procedure described by Vanderplaats and used in the optimization program ADS [8]. Inequality constraints are also formulated for upper and lower bounds on α_e.

A minimum-change objective function is given by:

$$f(\{\alpha_e\}) = \sum_{e=1}^{p} (\alpha_e)^2, \tag{6}$$

where $\{\alpha_e\}$ is the vector of element change properties α_e. Alternatively, the function to be minimized could be minimum weight. For a system of uniform density, this function is given by:

$$f(\{\alpha_e\}) = \sum_{e=1}^{p} A_e \alpha_e, \tag{7}$$

where A_e is the element planform area perpendicular to the thickness.

The corrector examines the potential energy imbalance between the system output from the predictor and the desired system and corrects the imbalance through additional elemental changes. This enforces the natural frequency constraint on the ith mode:

$$\sum_{e=1}^{p} \left(\{\psi'\}_i^{\mathrm{T}} \left[\tilde{k}_e\right] \{\psi'\}_i - \omega_i'^2 \{\psi'\}_i^{\mathrm{T}} [m_e] \{\psi'\} \right) \alpha_e = \omega_i'^2 \{\psi'\}_i^{\mathrm{T}} [M] \{\psi'\}_i - \{\psi'\}_i^{\mathrm{T}} [K] \{\psi'\}_i, \tag{8}$$

where $\{\psi'\}_i$ is the perturbed eigenvector, ω_i' is the desired eigenvalue, and $[K]$ and $[M]$ are the global stiffness and mass matrices, respectively, and

$$[\tilde{k}_e] = [k_{e_{\text{memb}}}] + [k_{e_{\text{diff}}}] + 3[k_{e_{\text{bend}}}]. \tag{9}$$

The perturbed eigenvectors may be obtained in one of two ways. The first method, mentioned above, is to simply rerun the predictor. This yields the full, nonlinearly perturbed matrix of eigenvectors and the desired mode can be easily partitioned out. The second procedure involves the application of the following equation, where the change to the kth degree of freedom for the ith mode is:

$$\Delta\psi_{ki} = \sum_{e=1}^{p}\left\{\sum_{j=1}^{n}\left[\frac{\psi_{kj}}{M_j(\omega_i^2-\omega_j^2)}\left\{\{\psi\}_j^{\mathrm{T}}\left([k_{e_{\text{memb}}}]+[k_{e_{\text{diff}}}]\right)\{\psi\}_i\alpha_e + \{\psi\}_j^{\mathrm{T}}[k_{e_{\text{bend}}}]\{\psi\}_i(3\alpha_e+3\alpha_e^2+\alpha_e^3) - \omega_i^2\{\psi\}_j^{\mathrm{T}}[m_e]\{\psi\}_i\alpha_e\right\}\right]\right\} \quad (\text{for } j\neq i). \tag{10}$$

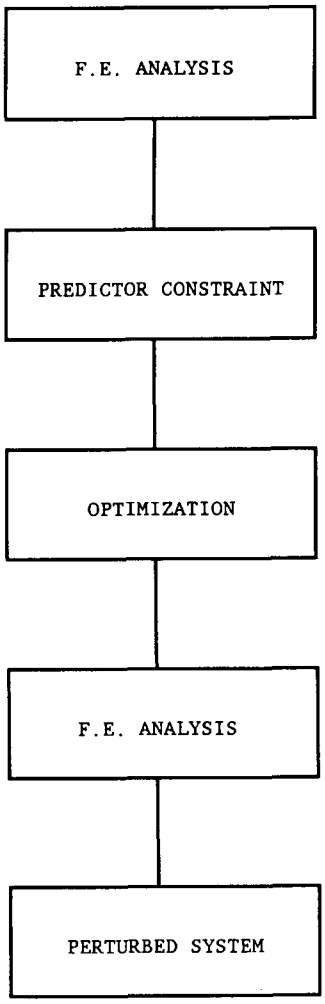

Fig. 2. Predictor overview.

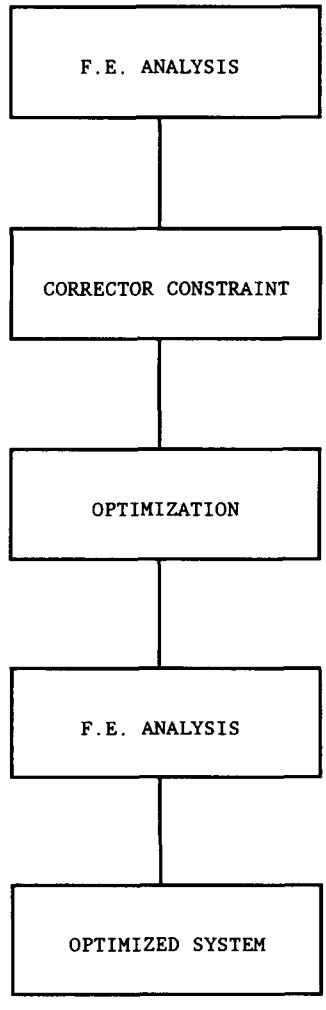

Fig. 3. Corrector overview.

This equation is a linear approximation of the perturbations in the eigenvectors. Using the results of reanalysis, one obtains the full, nonlinear changes in the eigenvector.

These two candidate procedures have definite trade-offs. Using eqn. (10) avoids another finite element run. However, eqn. (10) involves many matrix multiplications and manipulations and additional programing. Doing the reanalysis involves another finite element run, but it is simple to do and provides the exact intermediate answers. It also incorporates the changes in centrifugal force due to mass changes, which is something eqn. (10) cannot do. As a side benefit, the intermediate result of the predictor method alone is provided.

Overviews of the predictor and corrector are given in Figs. 2 and 3, respectively. For the predictor, the finite element solver is first run, to generate the system structural matrices and the eigenvectors. Then, using this information, the equation of constraint for the predictor is used using the frequency change equation. This constraint is used in the next step, the optimizer. Optimization is accomplished with respect to minimum weight or minimum change. Finally, a finite element analysis is done to obtain the system matrices and eigenvectors for the perturbed system produced by the predictor. The corrector uses a similar procedure with the energy balance equation serving as the constraint.

Results

The next step is to use the above method on a complex problem. Figure 4 shows a finite element model for a curved rotating cantilevered blade. The blade is made of Inconel 718 steel, has a radius of 254.0 mm, a length of 69.34 mm, and rotates at a speed of 200 Hz. It has an angle of attack of 30 degrees and is modeled after a NACA 64 airfoil. The blade is 10% thick at the root and tapers to 5% thickness at the tip.

The finite elements are each divided into two superimposed subelements; one with membrane properties and one with bending properties. This finite element model has approximately 1000 degrees of freedom. In the corrector, the lower limit on α_e will be changed so that no region will have a thickness less than one-half of the thickness of the original region.

For the nonrotating system, the fundamental frequency is 7665.6 rad/s. For the rotating system including centrifugal effects, the fundamental frequency is 8380.2 rad/s. This implies a 9.32% increase in fundamental frequency due to the centrifugal effect. The first eigenvector is a flapping, or bending, mode and the second one is a twisting, or torsional mode.

The problem of the rotating blade was analyzed for two cases, one involving a minimum-change objective in the predictor and in the corrector and another case involving minimum-weight objective. In cases 1 and 2, a 10% increase in the fundamental eigenfrequency was desired, with the objective function for case 1 being minimum change and the objective function for case 2 being minimum weight. Results of both predictor and corrector are shown in Table 1. Note that the predictor results can be considered to be results from a linear, one-step analysis since the effect of redesign on the eigenvectors does not enter into the

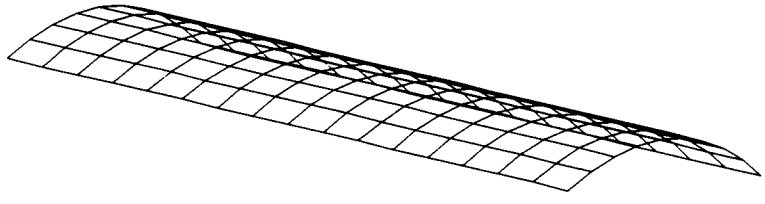

Fig. 4. Rotating blade.

Table 1
Optimization results for blade, 10% change

Case	Objective function [a]	ω_1 (rad/s)	ω_1^d (rad/s)	ω_1^P (rad/s)	$\%\Delta_p$	$\%\Delta W_p$	ω_1^c (rad/s)	$\%\Delta_c$	$\%\Delta W_c$
1	C/C	8380	9218	9246	103	4.09	9220	100	0.025
2	W/W	8380	9218	9210	99.1	−14.1	8948	67.7	−37.3

[a] C/C/: minimum change in both predictor and corrector steps; W/W: minimum weight in both steps.

predictor procedure. Improvements from the predictor-to-corrector step show the benefit of the use of the nonlinear optimization techniques.

In Table 1, the first column denotes the objective functions used in the predictor and the corrector respectively. The symbol C/C denotes minimum change in both steps. If W/W is indicated, minimum weight was used in both the predictor and corrector. The next heading ω_1 indicates the fundamental frequency for the system. The desired frequency is denoted by ω_1^d. The fundamental frequency resulting from the predictor geometry is indicated by ω_1^P. The percentage of the desired frequency change accomplished by the predictor is $\%\Delta_p$. The percent weight change resulting from the predictor is $\%\Delta W_p$. The fundamental frequency of the corrector geometry is ω_1^c. The percentage of the desired frequency change accomplished by the corrector is given by $\%\Delta_c$. In the final column, the percent weight change $\%\Delta W_c$ resulting from the corrector is given.

The final spanwise optimized thickness of the structure for Case 1 is given in Fig. 5 and for Case 2 in Fig. 6. Notice that in the minimum-change example (Case 1), emphasis is given to adding material at the root. In the minimum-weight example (Case 2), all of the regions except for the root have been reduced to the lower limit on thickness. This is the pathological case in optimization where the system is driven to an extreme. In this example, undesirable side effects occur, such as mode switching. The first bending mode is no longer the fundamental frequency and the the solution to the problem in optimization is no longer dependable. The frequency

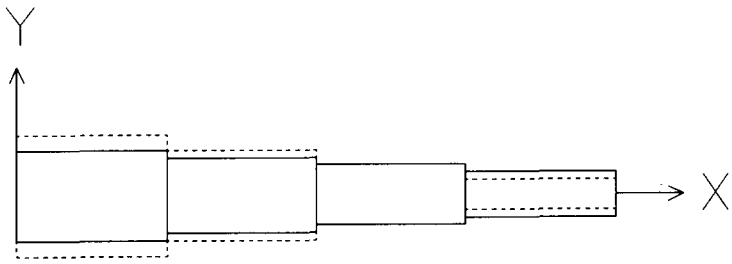

Fig. 5. Optimally redesigned blade, case 1: minimum change.

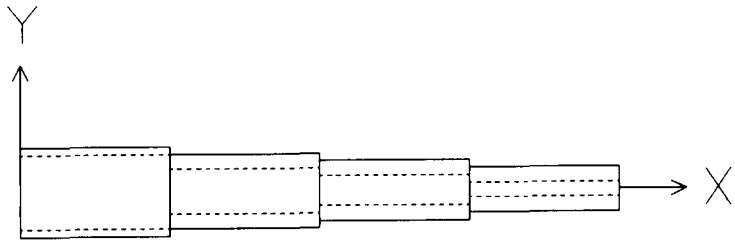

Fig. 6. Optimally redesigned blade, case 2: minimum weight.

Table 2
Optimization results for blade, 30% change; iterative procedure, minimum change

Case	Objective function	ω_1 (rad/s)	ω_1^d (rad/s)	ω_1^p (rad/s)	$\%\Delta_p$	$\%\Delta W_p$	ω_1^c (rad/s)	$\%\Delta_c$	$\%\Delta W_c$
3	C/C	8380	10890	11470	123	13.7	10920	101	9.80
4	C/C	10020	10890	10890	100	9.68	10890	100	9.68

Table 3
Optimization results for blade, 30% change; incremental procedure, minimum change

Case	Objective function	ω_1 (rad/s)	ω_1^d (rad/s)	ω_1^p (rad/s)	$\%\Delta_p$	$\%\Delta W_p$	ω_1^c (rad/s)	$\%\Delta_c$	$\%\Delta_c$
5	C/C	8380	9218	9246	103	4.09	9220	100	0.025
6	C/C	9220	10060	10080	103	8.62	10070	100	8.46
7	C/C	10070	10900	10910	102	13.7	10900	100	13.6

results shown for the corrector are for the bending mode; however, this frequency is technically no longer ω_1.

Two other problems were studied; both involved large (30%) changes in the fundamental frequency. In Case 3, the 30% change is accomplished in one step. A second iteration is performed to obtain an improved solution (Case 4). In another situation, the 30% change is broken down into three 10% increments (Cases 5–7). In all of these examples, only a minimum change objective function is used. Table 2 shows the results of the iterative procedure. The linear predictor step obtains the desired frequency change with 23% error,but at the end of the first design iteration, the desired frequency change is accomplished to within 1%. The second iteration is done for completeness, and gives the desired change in fundamental frequency to within 1/100 of 1%.

In Table 3, each increment obtains the desired change in frequency for that step to less than 1%. The final increment, which completes the 30% frequency change, gives the desired change to within 9/100 of 1%. These two tables show that excellent accuracy on the frequency goal is obtained, showing the feasibility of making large changes.

The use of the word "accuracy" needs some close examination. "Accuracy" has been used to describe how close the frequency change obtained by solving the problem in optimization is to the desired frequency change. This is done in terms of a discrete finite element model. Closed-form solutions to complicated structural systems are difficult to obtain. Therefore, in all discussions on accuracy, comparisons are made from one discrete model to another.

One of the reasons behind the lack of accuracy surrounding the problem of frequency control with minimum-weight objective is that this objective function in the presence of the nonlinear effects of the corrector drives most of the structure to the pathological extreme of the lower bound on thickness. This is an undesirable solution. Not only does it introduce inaccuracies that somewhat distance the frequency change from the desired value, but it also causes mode switching.

Conclusions

The predictor–corrector method for optimal redesign as extended in this dissertation obtained the desired frequency changes with excellent accuracy. MSC/NASTRAN finite element

solution sequences were modified to incorporate rotary effects. DMAP and FORTRAN languages were used to implement the derived equations of constraint. Automated Design Synthesis (ADS) was used to obtain the optimum solution. The methods used were applied to several test problems, one being a curved blade with nearly one thousand degrees of freedom. In each case, the desired frequency change was obtained to within a few percent. Therefore, the approach works and can be applied to a variety of problems in optimal redesign. The technology developed is transportable to other sites by anyone familiar with MSC/NASTRAN and DMAP.

References

[1] ZIENKIEWICZ, O.C., *The Finite Element Method,* McGraw Hill, London, 1977.

[2] COOK, R., *Concepts and Applications of Finite Element Analysis,* Wiley, New York, 2nd edn., 1974.

[3] HOFF, C.J., M.M. BERNITSAS, R.E. SANDSTRÖM and W.J. ANDERSON, "Inverse perturbation method for structural redesign with frequency and mode shape constraints", *AIAA J.* **22** (9) pp. 1304–1309, September 1984.

[4] STETSON, K.A., "Perturbation method of structural design relevant to holographic analysis", *AIAA J.* **13** (4), pp. 457–459, April 1975.

[5] STETSON, K.A. and G.E. PALMA, "Inversion of first-order perturbation theory and its application to structural design", *AIAA J.* **14** (4), pp. 454–460, April 1976.

[6] SANDSTRÖM, R.E. and W.J. ANDERSON, "Modal perturbation methods for marine structures", *Trans. Soc. Nav. Archit. Mar. Eng.* **90**, pp. 41–54, 1982.

[7] GANS, H.D., "Structural optimization including centrifugal and Coriolis effects", Ph.D. Thesis, The University of Michigan, Ann Arbor, MI, 1988.

[8] VANDERPLAATS, G.N., *ADS—A FORTRAN Program for Automated Design Synthesis (Version 1.10),* Engineering Design Optimization Inc., Santa Barbara, CA, 1985.